

# Constant amplitude fatigue test of high strength bolts in grid structures with bolt-sphere joints

Xu Yang<sup>a</sup> and Honggang Lei\*

College of Architecture and Civil Engineering, Taiyuan University of Technology,  
79 West Yingze Street, Taiyuan, Shanxi, People's Republic of China

(Received March 15, 2017, Revised June 02, 2017, Accepted August 29, 2017)

**Abstract.** The grid structure with bolt-sphere joints is widely adopted by industrial plants with suspending crane. The alternating reciprocating action of the suspending crane will cause fatigue problems of the grid structure with bolt-sphere joints with respect to the rod, the cone, the sealing plate, the bolt ball and the high strength bolt; while the fatigue of the high strength bolt is the key issue of fatigue failure. Based on efficient and smooth loading equipment with the AMSLER fatigue testing machine, this paper conducted a constant amplitude fatigue test on 18 M20 and 14 M30 high strength bolts with 40Cr material, and obtained 19 valid failure points, 9 unspoiled points with more than 2 million cycles, and 4 abnormal failure points. In addition, it established the constant amplitude fatigue design method,  $[\Delta\sigma]_{2 \times 10^6} = 58.91 \text{MPa}$ , and analyzed the stress concentration and the fatigue fracture of high strength bolts. It can be explained that the geometrical stress concentration of high-strength bolt caused by spiral burr is severe.

**Keywords:** fatigue test; grid structure; bolt sphere joint; high strength bolt connection; suspending crane

## 1. Introduction

A flat-grid structure with bolt-sphere joints rank is widely adopted in industrial plants due to advantages that include prefabrication and a robust but convenient construction.

In the past, the rated load on the hanging crane (as shown in Fig. 1) was not large with a maximum value of 10t. Recent innovations have resulted in significant improvements in this ratio, specifically, the rated load of the electric hoist generally ranges from 0.3t to 50t, and the working level is from M3 to M5 (JGJ7:2010, 2010). Whilst the rated load of the electric single-girder hanging crane ranges from 5t to 10t, and its working level is from A3 to A5 (JGJ7:2010, 2010); the rated load of the multi-pivot crane ranges from 1.0 t to 80t, and its working level is from A4 to A5 (JGJ7:2010, 2010); the daily operating speed is generally 20 ~ 30 m / min. The fatigue load caused by suspending crane should be paid attention to ensure structural safety. Scholars in different countries have different opinions as to whether it is necessary to consider the fatigue issue of the suspending crane on the large-span hangar (Jiao 2013). Some hangar designers in Britain argued that fatigue does not need to be considered.

However, the economic and social development is getting much closer with the international exchanges, and the maintenance hangar becomes more and more important.

Here in, two typical engineering examples of the maintenance hangar are considered.

The building area of the maintenance hangar is about 7700 m<sup>2</sup>, it adopts a grid structure, with bolt-sphere joints as the roof, with 108 m in span and 52.5 m for width. Two sets of 10t suspension bridge cranes are hung from the bottom chord of the hangar roof. There are 40 m for the width direction of the crane stroke, 104 m for the longitudinal direction, parameters that can cover all positions in the hangar. During the operation of the suspending crane, the entire grid vibrates frequently (Ba 2014).

The A380 hangar of Beijing Capital International airport was completed in March 2008. The span for the hall of the maintenance hangar is 176 m+176 m, the net span is 350.8 m, and the spatial depth is 110 m. The hangar can provide capacity for a total of 11,500 runs annually. The hall of the hangar is equipped with 2 sets of 15t cranes, 2 sets of suspension lifting platforms, and 1 set of crane span structure. The crane and the suspension lifting platform could cross the rail at any point, so as to serve the entire hangar hall and meet the maintenance requirements of each flight. The suspending crane is used frequently (Zhu *et al.* 2008).

The above maintenance hangars are widely used in the buildings with a similar grid structure. The working parameters, the rated load and the frequency of use of the crane equipment hanging on the grid structure have increased significantly, due to the rapid expansion of the global civil aviation sector and the exponential growth in the need for aircraft maintenance that this has resulted in such increased use places a great strain on the tolerance levels of the structure, and its life expectancy, as such particular attention should be paid to the hanging crane, as its constant vibration can cause fatigue problems in the bolt-

\*Corresponding author, Professor,  
E-mail: [lhgang168@126.com](mailto:lhgang168@126.com)

<sup>a</sup> Ph.D.,  
E-mail: [ganlanshu2054@163.com](mailto:ganlanshu2054@163.com)

sphere joints of the grid structures (Lei 2008).

One industrial plant complete with suspending crane was built in 2003. The roof uses a square pyramid grid structure with bolt-sphere joints. On May 16, 2015, the southwest corner of the grid structure suddenly collapsed, when the upper chord node bolt at the base of an angle area fractured, resulting in two chords close to the two spans of the base to lose stability. Three days later, the whole two-span grid on the west side collapsed, because the high strength bolt of the bolt-sphere joints failed due to fatigue damage caused by the long-term crane load. As shown in Figs. 2 and 3.



Fig. 1 Grid-structure industry workshop with hanging crane



Fig. 2 Bolt-sphere joint entities



Fig. 3 The accident for the grid structure

The fatigue problems of the flat grid structure focus on the fatigue of joints. In recent years, both domestic and foreign scholars have carried out a series of theoretical and experimental researches on tolerance levels for similar bolt-sphere joints. This research has produced some notable achievements: results are summarized as follows.

The key factor involved in the flat-grid structure with the bolt-sphere joints centers on the fatigue of the high strength bolt that it contains. In recent years, domestic scholars have carried out more systematic researches in this field. Xu and Cui (1994) conducted a total of 13 uniaxial constant amplitude fatigue tests for the 40Cr high strength bolt M14, and obtained 13 valid sets of constant amplitude fatigue test data, as well as the corresponding S-N curve. In addition to this, with the help of the equipment such as the scanning electron microscope, metallographic analysis for the fatigue failure of the high strength bolt was also carried out.

Feng and Lin (1995) research processed the constant amplitude fatigue test on the specifications of the high strength bolt in the grid structure were M24 and M33. The resulting fatigue test obtained 21 valid sets of constant amplitude fatigue test data.

More recently, Zafari *et al.* (2016) examined the static and fatigue performance of resin injected bolts for a slip and fatigue resistant connection. Whilst Wang *et al.* (2016) research focused on a low cycle fatigue test of M12 and M16 bolted T-stub connections to HSS columns. The paper of de Jesus *et al.* (2015) investigated the fatigue of riveted and bolted joints made of puddle iron. Whilst Noda *et al.* (2016) focused on the effect of pitch difference between the bolt-nut connections upon the anti-loosening performance and fatigue life. The conclusion is that the relative errors between the two models are found to be less than 12%. Berto *et al.* (2016) research on the effect of hot dip galvanization on the fatigue behaviour of steel bolted connections. Ghorbani *et al.* (2016) research centered on the estimation of fatigue life in bolt clamped Al alloy 2024-T3 plates. Juoksukangas *et al.* (2016) presented research on the experimental and numerical investigation of fretting fatigue behavior in bolted joints. Tizani *et al.* (2014) research on Fatigue life of an anchored blind-bolt loaded in tension. D'Aniello *et al.* (2016) research on the monotonic and cyclic inelastic tensile response of European preloadable gr10.9 bolt assemblies. Guo *et al.* (2016) research on load-bearing capacity of occlusive high-strength bolt connections.

## 2. Experiment design and test procedure

### 2.1 Specimen design

Based on the relevant provisions of *Technical Specification for Space Frame Structures* (JGJ7:2010, 2010), the specimens and the materials of connecting required for the fatigue test on the grid structure with bolt-sphere joints should be considered. Specific details of this involves the material for the steel pipe and bolted sphere, these should meet the quality of Q235B as specified in *Carbon Structural Steels* (GB700:2006, 2006). In addition,

the quality of the bolt ball should meet the relevant provisions of the *Steel Grid Structure With Bolt-sphere Joints* (JG/T 10:2009, 2009) .

1. BS150 (abbreviation of Bolt Sphere, the diameter is 150 mm). During the fatigue test on a high strength bolt, it is very likely that the bolt threads will be damaged, or part of the cracked bolt will remain in the hole which cannot be removed. Therefore, in order to improve the utilization efficiency of the bolt ball, three pairs of threads were set in groups ( $\Phi 20-\Phi 20$  or  $\Phi 30-\Phi 30$ ) on each bolt ball, then, once one thread fails, the bolt could still carry out the fatigue test via reversing in direction. Thus, a bolt ball can be reused multiple times, see Fig. 4.

2. High strength bolt (HSB) M20 and M30. It is made of 40Cr, with performance rating of 10.9S. The appearance of each high strength bolt would be checked before the test, and the initial defective bolts would be recorded by using a number.



Fig. 4 Bolt sphere specimens



Fig. 5 Simulation of cone head

3. M20 and M30 specimen (simulation of cone head). At the end of the seamless steel pipe with  $450\text{ mm}\Phi 102 \times 7$  long is welded with the cone supporting the M20 or M30 high-strength bolt. According with the Article 5.3.7 provision in *Technical specification for Space Frame Structures* (JGJ7:2010, 2010), thus, truly reflecting the connection of the high strength bolt in the grid structure with bolt-sphere joints. At the other end, the hole is open, which could be connected with the support and the load beam. If the M20 or M30 bolt is damaged due to fatigue, a new bolt could be replaced to continue the test, see Fig. 5.

4. Support. Each group of loaded specimen is equipped with upper and lower supports with hole on each side, M20 and M30 have identical specimen holes, so that it could be connected with the upper and lower steel beams.

## 2.2 Test loading equipment

The success of a fatigue test is closely related to the suitability of the fatigue loading device. The rods of the grid structure are designed as axial force members, adopting the axial fatigue test would be a simple and reasonable task, and may greatly reduce the test cost. Therefore, the loading device was designed to suit this condition, and all the fatigue test specimens could be carried out on this device. The loading device is as follows (Fig. 6):

Test equipment: Amsler1200-type pulse fatigue test machine.

Pulse value: 400 cm<sup>3</sup> / min, five-speed.

Pulse Jack: 4 types including 50 KN / 100 KN, 100 KN / 200 KN, 250 KN / 500 KN, and 500 KN / 1000 KN.

Four gears contains 1/10, 1/4, 1/2, and 1 for the pendulum dynamometer meter range.

The two steel beams with a box shape are on the upper and the lower test loading frame, their symmetrical positions on both sides of the steel beam L2 are respectively fixed with a 50t hydraulic jack, and the intermediate position is connected with the steel beam L1 via the suspended test specimen. The two hydraulic jacks realized the cyclic tensile loading on the test specimen group by applying the cyclic compressive stresses to L1. As this study took the stress amplitude as a parameter, the self-balancing test device is both scientific and safe.

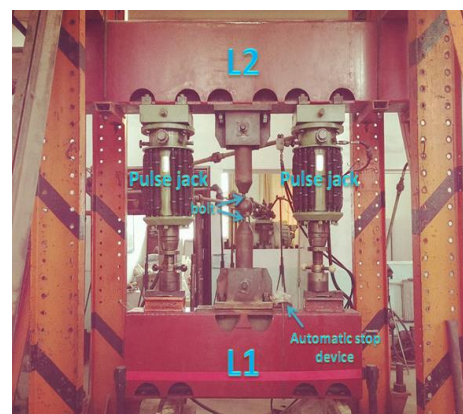


Fig. 6 Loading equipment

The central position of the steel beam on the steel frame is respectively fixed with an M20 or M30 high-strength bolt support, to connect the M20 or M30 specimen with the M20 or M30 bolt by the bolt ball. The load is applied by the two hydraulic jacks connected with the AMSLER fatigue test machine, and the pressure of the jacks is applied to the intermediate specimen group by the steel beam. Two high strength bolts could perform fatigue cycles simultaneously at any given time.

2.3 Constant amplitude fatigue test

Because of the inevitable deviation in the vertical direction or the hole position in the production of the specimen, the beam will swing out of plane, when the cyclic load is applied. In order to reduce the damage to the jack, as well as the impact on the accuracy of the test data, it is necessary to ensure that the specimen is upright and in the same plane as the load device in the fatigue test.

The stress ratio was set to be 0.3 with the above test device. According to the pre-established five load levels, the load would be loaded in accordance with its size order. The test procedures for the fatigue test of the 32 high strength bolts under constant amplitude load were:

1. Using the self-designed test loading device (Fig. 6), two high-strength bolts could be processed of the constant amplitude fatigue test each time. The specimen loading scheme would be determined based on the desired stress amplitude size, then the load is applied. During loading, the specimen and the test apparatus should be observed carefully and recorded in detail.

2. A "automatic stop device" is placed on the load beam L1. Thus, when the test device swings heavily, it will stop and a process of unload automatically. At this time, an examination of the conditions of the specimen and test equipment is carried out in order to ascertain which bolt is damaged due to fatigue.

3. To record the final number of the cycles of the bolt, and take pictures of the fatigue fracture, then to analyze the test information relating to specimen.

4. To replace the damaged bolt with a new one, and proceed to the next round of constant amplitude fatigue load and set a new stress amplitude and frequency. The previous undamaged bolt may be used as a specimen in this round of amplitude fatigue test specimen, and so on, then the amplitude fatigue loading test of high-strength bolt can be completed.

3. Test results

There were 6 M20 and 3 M30 high strength bolts load cyclic numbers with each exceeding  $2 \times 10^6$ , but the fatigue failure did not occur. In addition to this, 4 high strength bolts were found to contain different degrees of initial defects after inspection and the test data was deemed to be abnormal. Therefore, when the inclined portion of S-N curve was determined, 4 abnormal data should be excluded, then the valid data would be 19.

Through the regression analysis 19 valid fatigue test data,

the constant amplitude S-N curve of high strength bolts are shown in Figs. 7-10. And the equation formula for the corresponding part of the oblique line of the S - N curve in Figs. 9 and 10 is shown in Eqs. (1) and (2).

S-N curve equation

$$\lg N = 11.8459 - 2.6179 \lg(\sigma_{\max}) \pm 0.4796 \tag{1}$$

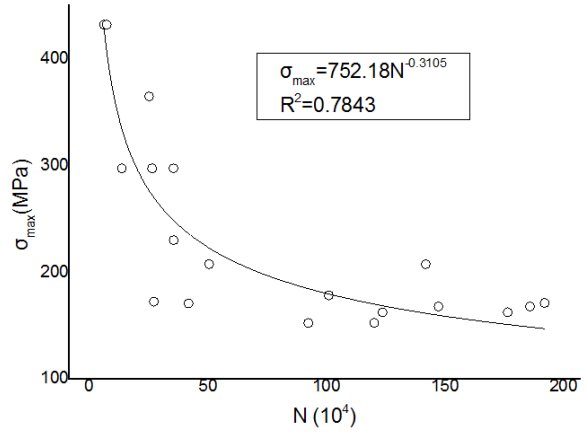


Fig. 7 The power regression curve takes the maximum stress as the parameter

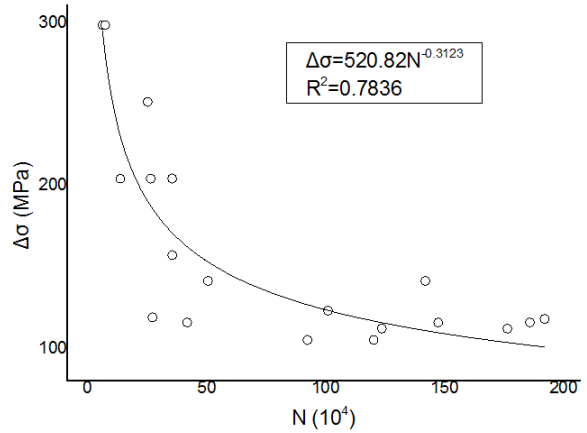


Fig. 8 The power regression curve takes the Δσ as the parameter

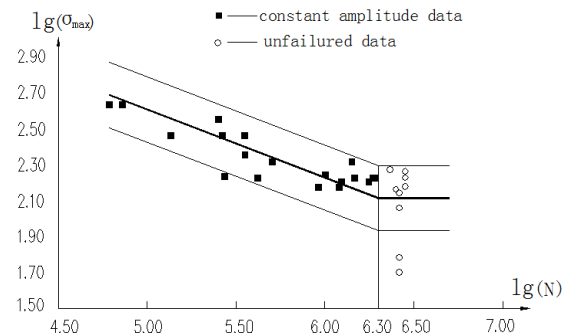


Fig. 9 The double logarithm regression curve with  $\lg \sigma_{\max}$  as the parameter

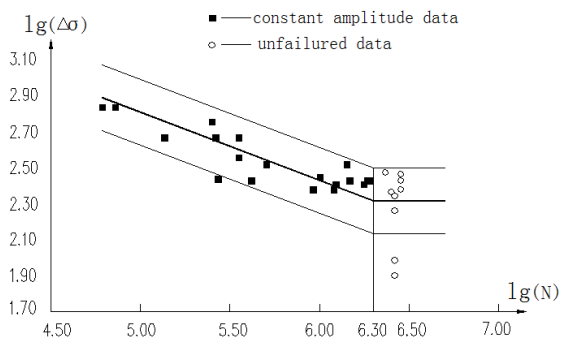


Fig. 10 The double logarithm regression curve with  $\lg\Delta\sigma$  as the parameter

Correlation coefficient

$$r = -0.8602; [\sigma_{\max}]_{2 \times 10^6} = 86.15 \text{MPa}$$

S-N curve equation

$$\lg N = 11.4005 - 2.6092 \lg(\Delta\sigma) \pm 0.4818 \quad (2)$$

Correlation coefficient

$$r = -0.8588; [\Delta\sigma]_{2 \times 10^6} = 58.91 \text{MPa}$$

#### 4. Defect characterization

This section attempted to carry out the macro and micro analysis on constant amplitude fatigue fracture of high-strength bolts obtained in the above fatigue test. This aimed to reveal the fatigue failure mechanism of high strength bolts in grid structures with bolt-sphere joints.



Fig. 11 M20-4 macro-view fracture

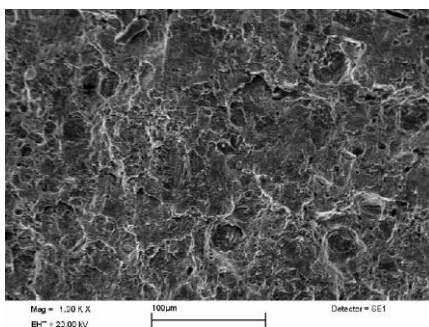


Fig. 12 M20-4 micro-view fracture (Source area)

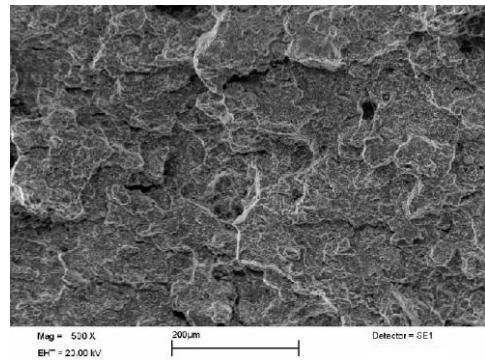


Fig. 13 M20-4 micro-view fracture (Extension region)

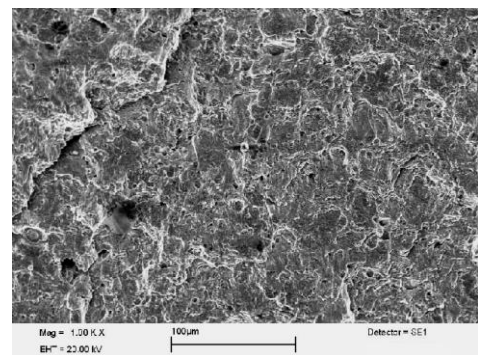


Fig. 14 M20-4 micro-view fracture (Transient zone)

The macro-view fracture shown in Fig. 11 that this fracture was cracked at a 45-degree angle. Through the analysis, it turned out that the bolt was not installed correctly which caused the bolt to bear some additional moment. Fig. 12 is a source area of 1000 times magnification, and no regular fatigue striations or radiation could be seen, more then, the stripes are messy. Fig. 13 is an expansion area of 500 times magnification, the obvious fatigue striations can be found. Fig. 14 is a transient zone that is enlarged 1000 times, and the torn marks of the sudden rupture could be seen.

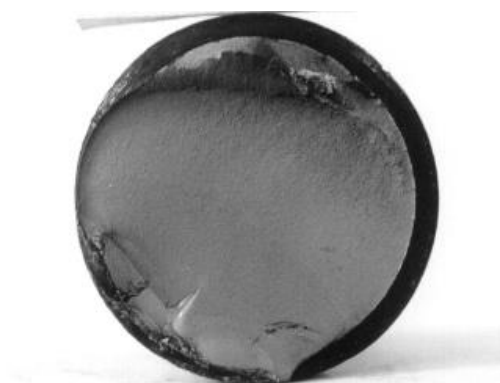


Fig. 15 M30-9 macro-view fracture

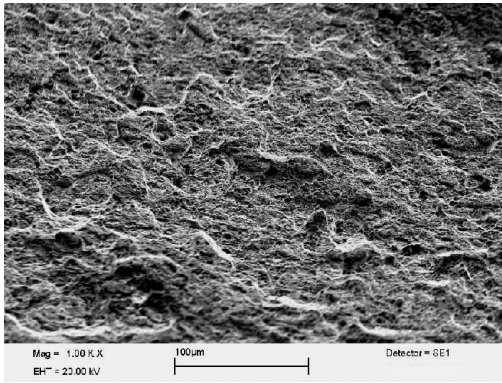


Fig. 16 M30-9 micro-view fracture (Original zone)

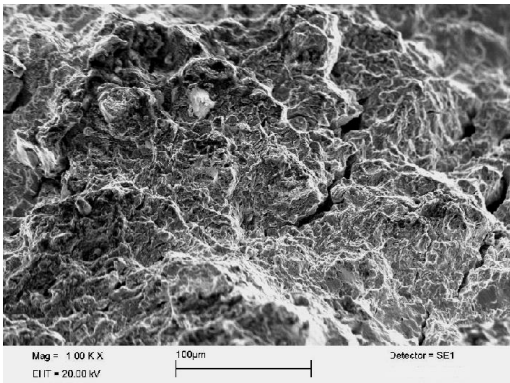


Fig. 17 M30-9 micro-view fracture (Developed zone)

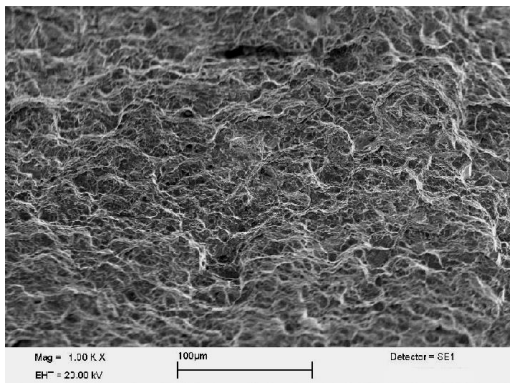


Fig. 18 M30-9 micro-view fracture (Transient zone)

It can find out from the macro-view fracture shown in Fig. 15 that this fracture cracks at the first screwed thread below the interface between the shank and the sphere. Moreover, there is only one fatigue source on the whole fracture surface, which is located at the lower thread. It's comparatively flat, and the middle crack extends along an obvious bay ridge. The Fig. 16 is a source area of 1000 times magnification, where it looks smoother than the other areas. The Fig. 17 is a developed zone of 1000 times magnification, with obvious radioactive rays. And the Fig. 18 shows the transient zone that is magnified 1000 times, where crystal particles are coarse on fracture and it's

obviously characterized with brittle fractures. In terms of appearance, this is a fatigue fracture obviously characterized with fatigue fracture in both macroscopic and microcosmic views.

Much macro-view and microscopic analysis on fractures of constant amplitude fatigue tests for high-strength bolt, the following conclusions can be drawn from the analysis of the process outlined above:

All fractures present typical fatigue failure characters, that is, fatigue fractures can be obviously divided into three regions: fatigue source region, extension area and transient zone. The detailed information of the three regions is listed as follows.

#### 1. Fatigue source region

Every fracture contains fatigue source regions. Some only contain one, whilst others contain several ones. The fatigue source region is most concentrated in the sections of the first thread of high-strength bolt. The first thread refers to the first exerted thread after high-strength bolt screwed in the bolted spherical joint, which displays the most severe concentration of stress. The fatigue source region is the source of fatigue failure. Through bay ridge of most fractures, fatigue source is the point of origin of bay ridge, mostly presenting half round or semi-ellipses shape at fractures. In terms of scale and sizes, compared with the extension area and transient zone, the fatigue source region occupies the smallest size among the whole fracture. Through pictures of microcosmic fracture, black specks or small specks obviously appeared in parts of the fatigue source region, which is inclusions in high-strength bolts, whose existence forms a concentration of stress, and is conducive to fatigue source. Also worthy of note are the obvious radioactive rays or fatigue striations that can be clearly seen nearby.

#### 2. Extension area

Every fracture has a crack extension area. The smoothness in extension area is not as honed as that in the source region, in which transparent fatigue striation is clearly visible ray hickey or striatum of bell curve focused on fatigue source. Also notable is the striatum of bell that is slightly waved extending forward centered on the fatigue source, which is also the biggest feature in the crack extension area. The shape of visible bay ridge is decided by its spreading rate, types of loading, degree of overloading and concentration of stress of each point along the line of cracks and other factors. It's much closer to fatigue source region, showing that the process of extension of the crack is relatively slow; far from the fatigue source region, the bay ridge is relatively sparse, showing that the extension of the crack in this section is relatively fast. As for the extension area with multiple sources of fatigue, cracks extend on planes favorable to their own development, and, with fatigue cracks extending on two different planes meet and connect with each other, it frequently forms a fatigue step or many long typical tearing edges through the ways of shearing or tearing, and cracks gradually develop on the same plane. In terms of variable-amplitude fatigue fracture, randomness of fracture is often much larger than that of variable-amplitude fatigue fracture.

### 3. Transient zone

Every fracture contains a transient zone, which is mostly located in the opposite side of its fatigue source. Its fracture appearance is much coarser and its shape is irregular when compared with fatigue source zone and its extension area. The fracture with a macro-scale character similar to a static crack presents radial or zigzag appearance in the middle-plane strain area. In edge plane, it presents shear lip stress block, showing sensible brittle fracture characteristics.

## 5. Finite element analysis

### 5.1 Fatigue failure mode

During the fatigue test on bolted spherical joint multi-grids two failure modes in the high-strength bolt appear.

The first failure mode involves high-strength bolt cracks at the first thread of occlusion between screw threads; as a result, it is clear and distinguishable to see the smooth fatigue area and coarse rupture region on the fractured surface, which is a typical feature of surface of fatigue break. In this test, this kind of crack form is the most typical of the form of fracturing that occurs in this kind of fatigue test. From this high incidence we can deduce that the main reasons causing this break form are: (1) the effective cross section of the high-strength bolt is located where its thread is the smallest, moreover, there is occlusion between the threaded rods that screw into both screwball and bolted spherical joints, as well as the tension that bolt bears that is shared by bolt and tightening latch that screws in the bolt, while the tension located at the thread occluded with the first screw thread under the surface of the bolted spherical joint is only endured by the tightening latch of the bolt, as a result, it leads to a level of stress that is comparatively high, and an increased probability of fatigue. (2) Since the stiffness of the bolted spherical joint is higher compared with the bolt, it is with a fixed effect on the bolt. In addition, it is because that uncompleted coincidence of the tie rod of manufacturing tolerance and initial eccentricity existing in test load and other factors would lead the bolt eccentric and under stress. Therefore, the stress due to bending is still the highest at the first thread of occlusion, between the tightening latch and the surface of the bolted spherical joint, where fatigue failure of bolted spherical joint multi-grids mainly happened, all in all.

Another notable failure mode appears in this test — fatigue fracture at transition between high-strength bolt tie rod and blind nut. This kind of failure mode only occurs twice in the test's duration. A great abrupt change of cross-section of bolt is characteristic of this form of fracture, and we can attribute this as the main reason to produce the fatigue fracture. Therefore, as for the high-strength bolt located at support of hanging point of hanging crane, it's suggested to replace the high-strength bolt with few abrupt changes of cross-section with the high-strength bolt with ordinary blind nut, which is a very effective measure to improve its fatigue strength, avoiding the happening of this kind of breaking.

### 5.2 Stress concentration analysis

According to the above two fatigue failure fracture forms; this article makes an analysis on this modeling of test specimens with ABAQUS.

Model parameter configuration, elasticity modulus: high-strength bolt  $E=2.11 \times 10^5 \text{MPa}$  (40Cr); Bolted spherical joint  $E=2.11 \times 10^5 \text{MPa}$  (45 type steel); Poisson's ratio: 0.3; Applied P: 100MPa. Application of reinforcement of end constraints of the ball section, Standard: High-strength bolt M20 (triangular thread); bolted spherical joint:  $D=150 \text{mm}$ .

The whole model is shown in the Fig. 19.

The analytical result is shown in the Figs. 20-23.

From the above analytical result: the stress that the bolt is located at thread is relatively high, and stress distribution and stress concentration are the most obvious at the first thread between bolted spherical joint and bolt mesh.

Taking the first root fracture surface as stress — path graph and stress-path graph of making vertical surface of bolt, as is shown in the Figs. 24 and 25.

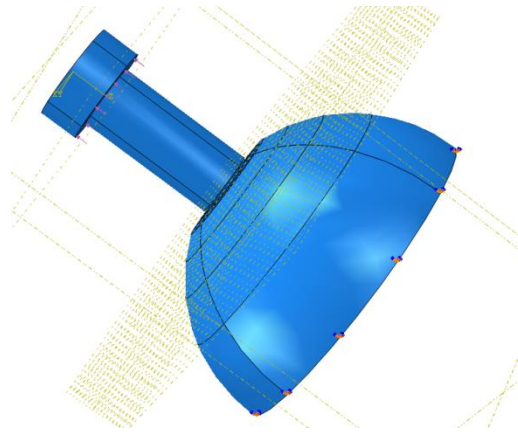


Fig. 19 Bolt ball and loading ways of the mesh and the overall model of bolt

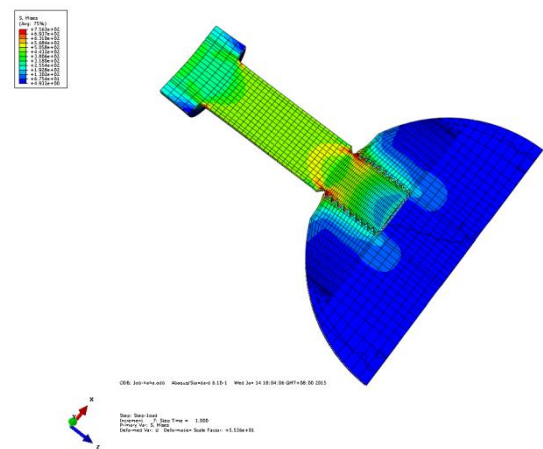


Fig. 20 Bolt ball and the cross section of mises stress nephogram

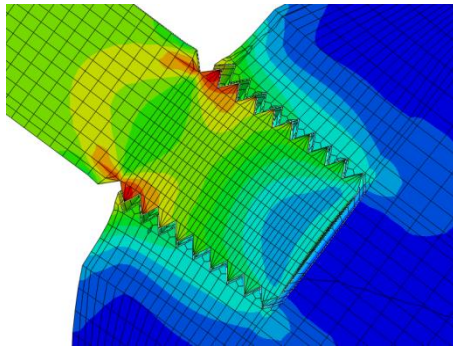


Fig. 21 Detail of mesh to the ball in the thread mises stress cloud

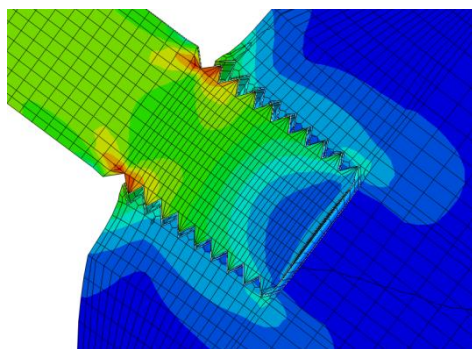


Fig. 22 Meshing thread strain contours of the ball

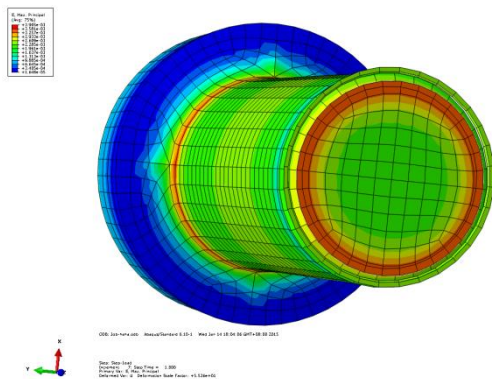


Fig. 23 The first tooth root stress nephogram of area

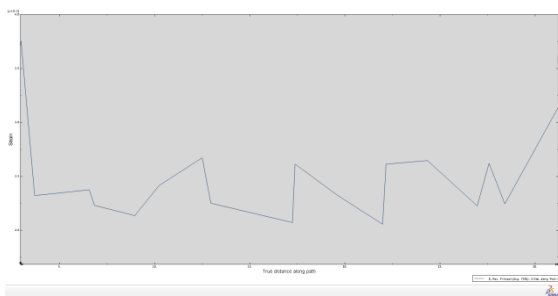


Fig. 24 The first root section stress - path graph

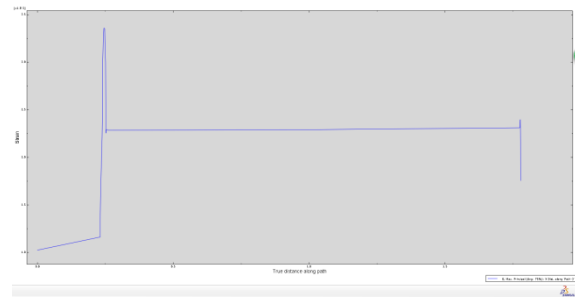


Fig. 25 Bolt stress profile - path graph

From the above analysis: the stress is relatively high at the first root close to gap, which explains that the ratio of concentration of stress at the gap is highest.

From the above analysis, it's known that the stress of bolt between mesh and bolted spherical joint is relatively low because of constraint function of bolted spherical joint.

The closer to the surface of the bolted spherical joint, the higher the stress is. And it achieves the highest value at the first root between the bolt to the bolted spherical joint; In the part of smooth tie rod, it keeps stress stable; and in the joint of tightening latch and blind nut, there appears the phenomenon of concentration of stress. Due to excessive smooth between tightening latch and blind nut, on which the concentration of stress is relatively lower compared with that of the thread. From above analysis and large amounts of data, it shows that fatigue undermine mainly happens first between the bolt and the bolted spherical joint mesh, where the concentration of stress is the most obvious. Therefore, as a model, it is feasible to carry on analysis on the concentration of stress of single spiral burr, and it proves that the data of this experiment is dependable.

### 5.3 Calculating method for constant amplitude fatigue

Through a large number of tests, it shows that the main factor affecting high-strength bolt fatigue strength in latticed frame with bolted balljoints under suspended crane loading is stress amplitude other than stress ratio and maximum stress. So, this article takes  $\Delta\sigma$  as its design parameter, adopting allowable stress amplitude method, the established bolted spherical joint multi-grids using constant amplitude fatigue of high-strength bolt computational method as follows:

The checking formula is

$$\Delta\sigma \leq [\Delta\sigma] \tag{3}$$

$$[\Delta\sigma] = \left( \frac{C}{N} \right)^{1/\beta} \tag{4}$$

In this equation:

$\Delta\sigma$  — the maximum stress amplitude of the calculation of high-strength bolt;

$\Delta\sigma = \sigma_{\max} - \sigma_{\min}$ ;

$\sigma_{\max}$  — the maximum stress of the calculation of high-

strength bolt;

$\sigma_{\min}$ —the minimum stress of the calculation of high-strength bolt;

$[\Delta\sigma]$ —the allowable stress amplitude of high-strength bolt;

If it takes  $N=2\times 10^6$  as the base period, then  $[\Delta\sigma]_{2\times 10^6}=58.91\text{MPa}$ ;

$N$ —number of cycles

$C$ 、 $\beta$ —parameters, according to the S—N curve of Eq. (2),  $C$ 、 $\beta$  are separately taken as  $1.3326\times 10^{10}$  and 2.4876, respectively.

## 6. Conclusions

This paper conducted fatigue test of constant amplitude on 32 high-strength bolt fatigue test pieces with M20 and M30 specification. And then it obtained 19 valid failure points, 4 abnormal failure points and 9 unspoiled points over  $2\times 10^6$ .

• After conducting fatigue test of constant amplitude on 32 high-strength bolt fatigue test pieces with high strength bolts, the correspondent S—N curve equation obtained is:

$$\lg N = 11.4005 - 2.6092 \lg(\Delta\sigma) \pm 0.4818$$

Correlation coefficient:  $r = -0.8588$ ;  $[\Delta\sigma]_{2\times 10^6} = 58.91\text{MPa}$ .

• Taking  $\Delta\sigma$  as the design parameter, adopting allowable stress amplitude method, the constant amplitude fatigue computational method of high-strength bolt for the grid structure with bolt-sphere joints is established, it provides the basis for the designers.

## Acknowledgments

This project was supported by the National Natural Science Foundation of China (Grant No.51578357 and No.51178286).

## References

- Ba, S. (2014), "Repair of an aircraft hangar space truss design", *Comput. Knowledge Technol.*, **10**(20). (in Chinese)
- Berto, F., Mutignani, F. and Guido, E. (2016), "Effect of hot dip galvanization on the fatigue behaviour of steel bolted connections", *Int. J. Fatigue*, **93**, 168-172.
- D'Aniello, M., Cassiano, D. and Landolfo, R. (2016), "Monotonic and cyclic inelastic tensile response of European preloadable gr10.9 bolt assemblies", *J. Constr. Steel Res.*, **124**, 77-90.
- de Jesus, A.M.P., Da Silva, A.L.L. and Correia, J.A.F.O. (2015), "Fatigue of riveted and bolted joints made of puddle iron—An experimental approach", *J. Constr. Steel Res.*, **104**, 81-90.
- Feng, X. and Lin, X. (1995), "Fatigue performance under suspension crane action of bolt ball grid nodes", *J. Build. Struct.*, **16**(4), 3-12. (in Chinese)
- GB50017 (2003), *Code for Design of Steel Structures*, Beijing, China.
- GB700 (2006), *Carbon Structural Steels*, Beijing, China.
- Ghorbani, H., Chakherlou, T.N. and Taghizadeh, H. (2016), "On the estimation of fatigue life in bolt clamped Al-alloy 2024-T3

plates", *Eng. Fract. Mech.*, **164**, 74-92.

- Guo, X., Zhang, Y., Xiong, Z. and Xiang, Y. (2016), "Load-bearing capacity of occlusive high-strength bolt connections", *J. Constr. Steel Res.*, **127**, 1-14.
- JG/T 10 (2009), *Bolted Spherical Node of Space Grid Structures*, Beijing, China.
- JGJ7 (2010), *Technical Specification for Space Frame Structures*, Beijing, China.
- Jiao, J. (2013), "The theoretical and experimental research on fatigue performance of crossed plate-welded hollow spherical connection in plate-type grid structure", Ph.D. Dissertation, Taiyuan University of Technology, China.
- Juoksukangas, J., Lehtovaara, A. and Ntyl, A. (2016), "Experimental and numerical investigation of fretting fatigue behavior in bolted joints", *Tribol. Int.*, **103**, 440-448.
- Lei, H. (2008), "The theoretical and experimental research on fatigue performance of high strength bolt connection in grid structure with bolt sphere joint", Ph.D. Dissertation, Taiyuan University of Technology, China.
- Noda, N.A., Chen, X., Sano, Y., Wahab, M.A., Maruyama, H., Fujisawa, R. and Takase, Y. (2016), "Effect of pitch difference between the bolt-nut connections upon the anti-loosening performance and fatigue life", *Mater. Design*, **96**, 476-489.
- Tizani, W., Rahman, N.A. and Pitrakkos, T. (2014), "Fatigue life of an anchored blind-bolt loaded in tension", *J. Constr. Steel Res.*, **93**, 1-8.
- Wang, Z., Wang, Q., Xue, H. and Liu, X. (2016), "Low cycle fatigue response of bolted T-stub connections to HSS columns — Experimental study", *J. Constr. Steel Res.*, **119**, 216-232.
- Xu, G. and Cui, J. (1994), "Grid structure fatigue and fatigue life calculation", *J. Build. Struct.*, **15**(2), 25-34. (in Chinese)
- Zafari, B., Qureshi, J., Mottram J.T. and Rusev, R. (2016), "Static and fatigue performance of resin injected bolts for a slip and fatigue resistant connection in FRP bridge engineering", *Structures*, **7**, 71-84.
- Zhu, D., Pei, Y., Xu, R., Tang, H., Zeng, D. and Zhao, T. (2008), "Design and research on the long-span structure of Beijing A380 hangar", *China Civil Eng. J.*, **41**(2), 1-8. (in Chinese)

CC